AMERICAN SOCIETY FOR MICROBIOLOGY | Applied and Environmental Microbiology®

GENETICS AND MOLECULAR BIOLOGY

Experimental Evolution of *Escherichia coli* K-12 at High pH and with RpoS Induction

Issam Hamdallah,[a,b] Nadia Torok,[a] Katarina M. Bischof,[a] Nadim Majdalani,[b] Sriya Chadalavada,[a] Nonto Mdluli,[a] Kaitlin E. Creamer,[a] Michelle Clark,[a] Chase Holdener,[a] Preston J. Basting,[a] Susan Gottesman,[b] Joan L. Slonczewski[a]

[a]Department of Biology, Kenyon College, Gambier, Ohio, USA

[b]Laboratory of Molecular Biology, National Cancer Institute, National Institutes of Health, Bethesda, Maryland, USA

ABSTRACT Experimental evolution of *Escherichia coli* K-12 W3110 by serial dilutions for 2,200 generations at high pH extended the range of sustained growth from pH 9.0 to pH 9.3. pH 9.3-adapted isolates showed mutations in DNA-binding regulators and envelope proteins. One population showed an IS*1* knockout of *phoB* (encoding the positive regulator of the phosphate regulon). A *phoB*::*kanR* knockout increased growth at high pH. *phoB* mutants are known to increase production of fermentation acids, which could enhance fitness at high pH. Mutations in *pcnB* [poly(A) polymerase] also increased growth at high pH. Three out of four populations showed deletions of *torI*, an inhibitor of TorR, which activates expression of *torCAD* (trimethylamine *N*-oxide respiration) at high pH. All populations showed point mutations affecting the stationary-phase sigma factor RpoS, either in the coding gene or in genes for regulators of RpoS expression. RpoS is required for survival at extremely high pH. In our microplate assay, *rpoS* deletion slightly decreased growth at pH 9.1. RpoS protein accumulated faster at pH 9 than at pH 7. The RpoS accumulation at high pH required the presence of one or more antiadaptors that block degradation (IraM, IraD, and IraP). Other genes with mutations after high-pH evolution encode regulators, such as those encoded by *yobG* (*mgrB*) (PhoPQ regulator), *rpoN* (nitrogen starvation sigma factor), *mall*, and *purR*, as well as envelope proteins, such as those encoded by *ompT* and *yahO*. Overall, *E. coli* evolution at high pH selects for mutations in key transcriptional regulators, including *phoB* and the stationary-phase sigma factor RpoS.

IMPORTANCE *Escherichia coli* in its native habitat encounters high-pH stress such as that of pancreatic secretions. Experimental evolution over 2,000 generations showed selection for mutations in regulatory factors, such as deletion of the phosphate regulator PhoB and mutations that alter the function of the global stress regulator RpoS. RpoS is induced at high pH via multiple mechanisms.

KEYWORDS evolution, high pH, PhoB, RpoS

Escherichia coli is a neutralophilic bacterium with the ability to grow under a wide range of pH. Before colonizing the colon, the bacteria survive exposure to acidic levels as low as pH 2.0 in the stomach and alkaline levels exceeding pH 10 at the pancreatic duct (1, 2). During growth, *E. coli* normally maintains a cytoplasmic pH within the range of pH 7.4 to 7.9 (3, 4), while growing over the range of external pH 5.0 to 9.0 (5). At high external pH, the cell downregulates expression of acid stress response genes and positively regulates expression of base resistance genes (6, 7). The acid-inducible phosphate regulator PhoB limits production of fermentation acids; *phoB* deletion thus increases acid production, which could enhance cell growth at high pH (8, 9). A different response involves the NhaA Na^+/H^+ antiporter, which imports

Received 2 March 2018 **Accepted** 14 May 2018

Accepted manuscript posted online 25 May 2018

Citation Hamdallah I, Torok N, Bischof KM, Majdalani N, Chadalavada S, Mdluli N, Creamer KE, Clark M, Holdener C, Basting PJ, Gottesman S, Slonczewski JL. 2018. Experimental evolution of *Escherichia coli* K-12 at high pH and with RpoS induction. Appl Environ Microbiol 84:e00520-18. https://doi.org/10.1128/AEM.00520-18.

Editor Rebecca E. Parales, University of California, Davis

Address correspondence to Joan L. Slonczewski, slonczewski@kenyon.edu.

I.H. and N.T. contributed equally to this article.

protons in exchange for sodium ion at high external pH. The *nhaA* gene is upregulated at high pH (10, 11).

Another way that *E. coli* acclimates to pH stress is by inducing the global stress sigma factor *rpoS*, which regulates ~500 stress-associated genes and 1,044 genes in total (12, 13). RpoS is expressed at high levels under a variety of stress conditions, such as nutrient starvation associated with stationary phase (14), as well as during exponential phase if the cells face other external stresses such as temperature shock, osmotic stress, or acid stress (12). RpoS function is required at extremely high pH (pH 9.8), where cells cannot grow but remain viable (15).

The mechanism of the RpoS contribution to the high-pH stress response is unknown. RpoS expression is regulated via transcription, translation, and proteolysis. Transcriptional upregulation or mRNA stabilization may be stimulated by the alarmone (p)ppGpp and is negatively regulated by the cAMP-cAMP receptor protein (cAMP-CRP) complex (16). Translation of *rpoS* is regulated by small regulatory RNAs (sRNAs) (12, 17). Inhibition of proteolysis is an additional means by which RpoS levels are elevated when cells encounter stress (16). When cells are growing well, adaptor protein RssB takes RpoS to the ClpXP protease for degradation (18). However, during stress, antiadaptors IraM, IraP, and IraD sequester RssB, thereby stabilizing RpoS; each antiadaptor is induced under a different stress condition (19).

At high pH in the gut environment, enteric bacteria face anaerobic conditions under which ATP synthesis is less than optimal. One system that enables bacteria to compete under both alkaline and anaerobic conditions is *torCAD* (20). The *torCAD* respiratory operon is induced in the presence of trimethylamine *N*-oxide (TMAO); the resulting proteins reduce TMAO to trimethylamine (TMA) under regulation by the periplasmic TorT protein and the two-component TorS histidine kinase and TorR response regulator (21). Production of trimethylamine alkalizes the extracellular medium (20). Another target of TorR, the tryptophan deaminase TnaA, may help the cell to anticipate and deal with alkaline stress (5, 6, 20). The *torCAD* operon is negatively regulated by TorI, a transcriptional regulator that originated as the excisionase of defective prophage KplE1 (22).

We devised an evolution experiment to select for mutations that enhance growth and/or stationary-phase persistence at high pH. We cultured *E. coli* W3110 at the upper limits of pH base stress (pH 9.0 to pH 9.3) for 2,200 generations in a 96-well microtiter plate and then sequenced (Illumina MiSeq 2 × 250) the genomes of two clones from each of four individual population wells (B11, F7, D9, and G9). Mutations were predicted by reference-based alignment using the computational pipeline breseq 0.30.0 (23). Previous laboratory evolution experiments have adapted *E. coli* to grow optimally in various stressful environments and have identified novel mutations that confer higher fitness in external acid, permeant acid, and minimal media (24–26). A common mechanism of evolution involves mutation of regulators that shift expression levels of many genes in complex ways, such as the Gad regulon at low pH (27).

In this paper, we present a genetic basis for adaptation under prolonged exposure to alkaline stress under semiaerobic conditions. Our studies reveal high-pH fitness advantages for mutations in regulatory genes such as *phoB* (activator of phosphate regulon) (8, 9) and in components affecting expression of *rpoS*.

RESULTS

The fitness of populations (B11, F7, D9, and G9) increases at pH 9.25. At pH levels above approximately pH 9.0, our *E. coli* strain W3110 grows for approximately four doublings, and then the culture declines without achieving sustained stationary phase. We began subculturing 24 populations of W3110 *E. coli* at pH 9.0, near the upper limit for sustained growth. The evolving cultures reached progressively higher endpoint densities (Fig. 1). As the endpoint density increased, the pH of the medium was increased to pH 9.2 (470 generations), then to pH 9.25 (1,200 generations), and finally to pH 9.3 (1,900 generations). After 2,200 generations, the stationary-phase culture density at pH 9.25 was more than 3-fold higher than that of the ancestral strain. This

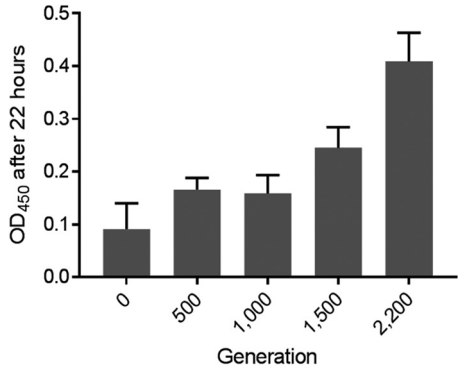

FIG 1 Endpoint growth of evolved populations from generations 0, 500, 1,000, 1,500, and 2,200 at pH 9.25. Frozen plates of evolved populations were thawed and diluted 1:50 into fresh LBK (with 150 mM AMPSO; pH 9.25) and then incubated in a microplate reader at 37°C for 22 h with intermediate shaking and subsequent OD_{450} readings every 15 min. Optical density was measured at 16 h. Mean values are shown for 8 representative evolving populations. Error bars indicate standard error of the mean (SEM) ($n = 8$).

steady increase in tolerance of the stress condition is consistent with the pattern seen for evolved populations subcultured at low pH (24) or in the presence of benzoic acid (25).

Genomes of high-pH-evolved clones show mutations. After 2,200 generations, two clones from each of four populations (B11, F7, D9, and G9) were isolated for genome sequencing (Tables 1 and 2). The sequences were aligned with the sequence determined from NCBI sequence NC_007779.1 for strain W3110; mutations found in our lab stock culture of strain W3110 were excluded from analysis. Populations F7 and D9

TABLE 1 Strains generated by experimental evolution, by P1 construction, or by recombineering

Strain	Population isolate	Description or genotype	Reference[a]
W3110		*Escherichia coli* K-12	
JLSH001	B11-1	W3110 evolved at pH 9.25	This study
JLSH002	B11-2	W3110 evolved at pH 9.25	This study
JLSH003	F7-1	W3110 evolved at pH 9.25	This study
JLSH004	F7-2	W3110 evolved at pH 9.25	This study
JLSH005	D9-1	W3110 evolved at pH 9.25	This study
JLSH006	D9-2	W3110 evolved at pH 9.25	This study
JLSH007	G9-1	W3110 evolved at pH 9.25	This study
JLSH008	G9-2	W3110 evolved at pH 9.25	This study
JLS1307		W3110 Δ*rpoS*::*kanR*	This study
JLS1622		W3110 Δ*torI*::*kanR*	This study
JLS1628		W3110 Δ*torR*::*kanR*	This study
JLS1714		JLSH007 (G9-1) Δ*torR*::*kanR*	This study
JLS1728		W3110 Δ*torS*::*kanR*	This study
JLS1729		JLSH007 (G9-1) Δ*torS*::*kanR*	This study
JLS1775		JLSH007 (G9-1) Δ*torCAD*	This study
SG30013		DJ480 ($rpoS_{750}$::*lacZ* translational fusion)	46
INH5		SG30013 Δ*iraM*::*tet* Δ*iraD*::*zeo* Δ*iraP*::*kan*	This study
INH12		W3110 Δ*phoB*::*kanR*	This study
INH14		W3110 Δ*ydcI*::*kanR*	This study
INH16		W3110 Δ*pcnB*::*kanR*	This study
NM376		*nlpD-rpoS* promoter region −775 to +10 fused to *lacZ*	This study
NM378		*nlpD-rpoS* promoter region −620 to +10 fused to *lacZ*	This study
BA943		Cm-Cp_{17}-C125T mutant $rpoS_{477}$-*lacZ*	34
BA938		Cm-Cp_{17}-$rpoS_{477}$ *lacZ*	34
SG30018		SG30013; Δ*rssB*::*tet*	52
BA926		Cm-Cp_{17}-*lac-lacZ*	34
XTL241		W3110 $galK_{tyr145UAG}$ Δ*lacU169* [λ cI857 Δ(*cro-bioA*)] *gam*<>*cat sacB*	53

[a]Strains indicated as created for this study are described further in Materials and Methods or elsewhere in the text (for evolved strains).

TABLE 2 Mutations found in selected populations after 2,200 generations at pH 9.1 to 9.3[a]

Position	H001 B11-1	H002 B11-2	H003 F7-1	H004 F7-2	H005 D9-1	H006 D9-2	H007 G9-1	H008 G9-2	Mutation	Annotation	Gene	Description
55,132									T→A	S660C (AGC→TGC)	*imp* ←	Exported protein for envelope biosynthesis
83,859									IS5 +4 bp	Intergenic (-151/-509)	*leuL* ← / → *leuO*	Leu operon leader peptide/transcrip. regulator
157,793									G→T	P445Q (CCG→CAG)	*pcnB* ←	Poly(A) polymerase I
345,978									IS +5 bp	Coding (271/276 nt)	*yahO* →	Periplasmic protein, YhcN family
416,368									IS1 +9 bp	Coding (3/690 nt)	*phoB* →	DNA-binding response regulator
584,703									IS +4 bp	Coding (151/954 nt)	*ompT* ←	Protease 7
663,577									C→T	G270D (GGC→GAC)	*dacA* ←	D-alanyl-D-alanine carboxypeptidase
664,261									G→A	P42L (CCG→CTG)	*dacA* ←	D-alanyl-D-alanine carboxypeptidase
716,294									G→T	C154F (TGC→TTC)	*ybfP* →	Hypothetical protein
1,154,102									C→T	T196M (ACG→ATG)	*fabF* →	3-Oxoacyl-[ACP] synthase II
1,154,222									C→T	A236V (GCC→GTC)	*fabF* →	3-Oxoacyl-[ACP] synthase II
1,222,922									IS +5 bp	Pseudogene (212/1115 nt)	Y75_RS06115 →	Autotransporter OMP
1,496,193									A→T	L198Q (CTG→CAG)	*ydcI* ←	DNA-binding transcriptional regulator
1,650,806									A→G	Intergenic (+51/-517)	*ydfC* → / → *dicB*	Hypothetical protein/cell division inhibitor
1,699,991									A→T	W302R (TGG→AGG)	*malI* ←	DNA-binding transcriptional repressor
1,739,985									T→A	V143E (GTG→GAG)	*purR* →	DNA-binding transcriptional repressor
1,910,446									IS + 5 bp	Coding (35/144 nt)	*yobG* ←	PhoP regulon feedback inhibitor MgrB
2,075,288									T→C	L538P (CTG→CCG)	*flu* →	Antigen 43 (Ag43) phase-variable biofilm
2,075,362									T→A	W563R (TGG→AGG)	*flu* →	Antigen 43 (Ag43) phase-variable biofilm
2,105,080									Δ7,823 bp		*insH*–[*rfbA*]	*insH*, Y75_RS10665, *wbbKJIH*, *glf*, *rfbX*, [*rfbCA*]
2,288,259									(TTATCGCCT)2→3	Coding (550/1761 nt)	*yejM* →	Hydrolase, inner membrane
2,424,139									IS5 +4 bp	Coding (484/543 nt)	*yfcD* ←	NUDIX hydrolase
2,471,831									Δ10,215 bp		*intS*–*torI*	*intS*, *yfd H I K L M N O P Q R S T J*, *torI*
2,523,563									Δ115 bp		[*alaW*]	tRNA-Ala(GGC)
2,689,918									C→T	Intergenic (-164/+394)	*yfhK* ← / ← *purL*	Sensory kinase phosphoribosylformyl-Gly-amide synth.
2,706,963									+C	Coding (448/957 nt)	*rseB* ←	Anti-sigma factor
2,759,692									IS +6 bp	Coding (490/627 nt)	*yfjJ* →	Hypothetical protein
2,779,908									A→C	V492G (GTA→GGA)	*ypjA* ←	Adhesin-like autotransporter
2,865,469									C→T	E247K (GAA→AAA)	*rpoS* ←	RNA polymerase, sigma S (sigma 38) factor
2,866,239									A→G	Intergenic (-32/+31)	*rpoS* ← / ← *nlpD*	RNA polymerase, sigma S (sigma 38) factor/OMP
2,944,225									G→A	R92C (CGT→TGT)	*ygdL* ←	Hypothetical protein
3,345,292									IS1 +10 bp	Coding (721/1434 nt)	*rpoN* →	RNA polymerase sigma-54 factor
3,377,221									C→A	D19Y (GAC→TAC)	*sspA* ←	Stringent starvation protein A; acid resistance regulator
3,511,182									G→A	D438N (GAC→AAC)	*priA* →	Primosome factor n'
3,542,266									A→C	Intergenic (+308/-143)	*rhaA* → / → *rhaD*	L-rhamnose isomerase/rhamnulose-1-phos. aldolase
3,542,284									T→C	Intergenic (+326/-125)	*rhaA* → / → *rhaD*	L-rhamnose isomerase/rhamnulose-1-phos. aldolase
3,609,245									A→C	Intergenic (+173/+208)	*fadA* → / ← *fre*	3-Ketoacyl-CoA thiolase/flavin reductase
3,688,524									A→C	H24Q (CAT→CAG)	*yjfE* ←	Hypothetical protein
3,883,308									G→A	E241K (GAA→AAA)	*yiaY* →	Fe-containing alcohol dehydrogenase
4,258,465									G→A	A531V (GCG→GTG)	*plsB* ←	Glycerol-3-phosphate O-acyltransferase
4,259,572									T→C	D162G (GAC→GGC)	*plsB* ←	Glycerol-3-phosphate O-acyltransferase
4,332,476									C→T	L222L (CTA→TTA)	*yjdA* →	Hypothetical protein
4,461,660									(TGGCAGAAG)2→1	(1196-1204/1374 nt)	*mpl* →	UDP-*N*-acetylmur:L-Ala-γ-D-Glu-m-diaminopim. ligase
4,546,841									IS +4 bp	(125/597 nt)	*fimE* →	Type 1 fimbriae regulatory protein FimE
4,547,155									G→A	A147T (GCG→ACG)	*fimE* →	Tyrosine recombinase/ *fimA* regulator
4,547,363									Δ1 bp	Intergenic (+50/-432)	*fimE* → / → *fimA*	Tyrosine recombinase/ *fimA* regulator/type 1 fimbrin
4,547,405									(T)6→5	Intergenic (+92/-390)	*fimE* → / → *fimA*	Tyrosine recombinase/ *fimA* regulator/type 1 fimbrin
4,635,602									C→T	L64F (CTT→TTT)	*slt* →	Lytic murein transglycosylase, soluble

[a]Two clones from each of four populations were selected and sequenced by Illumina MiSeq 2 × 250. The genomes were reassembled to the *E. coli* W3110 NCBI strain (accession number NC_007779.1) using breseq 0.30.0. Mutations affecting transcription of the lower strand involve the complement of the mutation that is listed. In the "Gene" column, arrows indicate direction of transcription. Gene mutation *ins-torI* includes loss of the KplE1 prophage. Letter colors: blue, missense mutation; green, silent mutation; red, substituted base position.

show several mutations in common, which might have arisen from inadvertent cross-transfer during an early time of serial culture.

The base-evolved sequences showed approximately 50 mutations in total from the eight sequenced strains compared to the ancestral W3110. These included 23 missense mutations but only one silent mutation, a ratio indicating a high likelihood of selection pressure. Insertion sequences (IS) caused 10 knockout mutations, as well as a large insertion-mediated deletion (*insH*-[*rfbA*]). The prevalence of IS-mediated knockouts is consistent with that reported for evolution experiments with acid stress (25, 27).

Three of the four populations (F7, D9, and G9) showed a deletion of prophage KplE1 (genes *intS-torI*), whose excisionase TorI functions also as a transcriptional regulator (28, 29). All four populations showed mutations related to *rpoS*, a known regulator of high-pH survival (15). Populations F7 and D9 shared a missense mutation, population B11 had a mutation upstream of *rpoS*, and population G9 showed a mutation in *sspA*, encoding an acid resistance protein that decreases H-NS expression and upregulates *rpoS* (30). Strain F7-1 showed a knockout insertion in *phoB*, the positive regulator of the

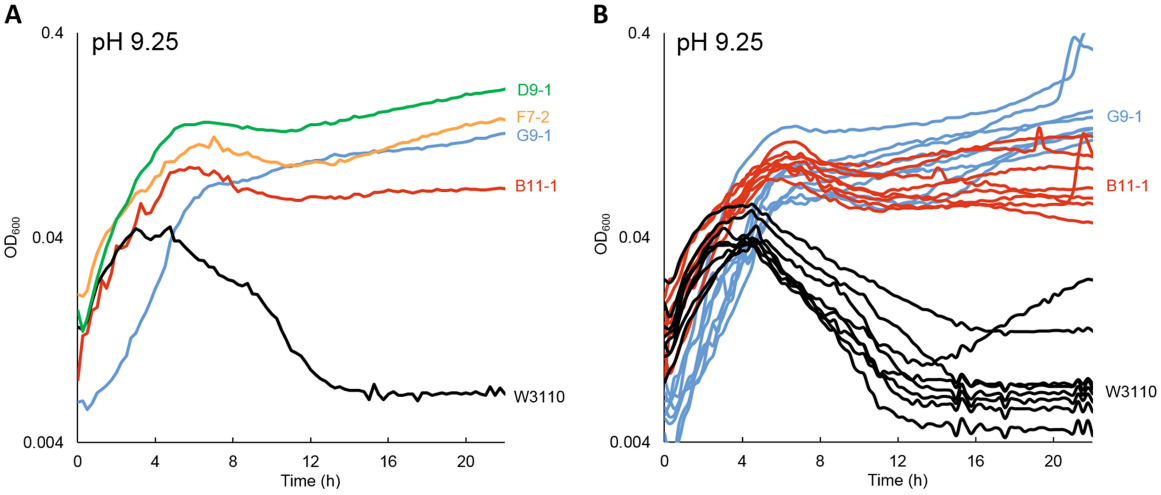

FIG 2 High-pH-evolved clones outgrow the ancestor W3110 at pH 9.25. Strains were cultured overnight at pH 8.5 as described in Materials and Methods. Overnight cultures were diluted 200-fold into microplate wells with LBK–150 mM AMPSO at pH 9.25; the final pH after 22 h of incubation was 9.15. (A) The curves shown have median OD_{600} values at 16 h. The 16-h culture densities of strains D9-1, F7-2, G9-1, and B11-1 showed a significant difference from that of the ancestral strain W3110 (Tukey test, $P < 0.05$). (B) Full set of 8 replicate growth curves for strains G9-1, B11-1, and W3110 from the same experiment as for panel A.

phosphate regulon (8, 9). Expression of *phoB* is induced at low pH, and *phoB* deletion increases production of fermentation acids. Other mutations found in the high-pH-evolved strains affected *rpoN* (encoding a nitrogen starvation sigma factor), *yobG* (*mgrB*) (PhoPQ regulator), *pcnB* [poly(A) polymerase], *ydcI* (transcriptional regulator), periplasmic and envelope protein genes (*imp*, *yahO*, and *ompT*); and murein maintenance enzyme genes (*mpl* and *slt*).

High-pH-evolved clones show a fitness increase at high pH but not at low pH. When cultured at pH 9.25, all the evolved clones (B11-1, F7-2, D9-1, and G9-1) grew to higher endpoint densities than did the ancestor W3110 (Fig. 2A). Early growth rates showed no significant differences, but the ancestor began to decrease in culture density after about 5 h in the alkaline medium, whereas the four evolved clones persisted in stationary phase. After 16 h of growth in pH 9.25 medium, evolved clones F7-2, D9-1, and G9-1 grew to a higher density than B11-1 (Tukey test, $P < 0.05$). For each strain, the curve shown is one of eight replicates showing the median culture density after 16 h of incubation. Figure 2B shows all eight replicates for two of the evolved strains, G9-1 and B11-1. Overall, our high-pH-adapted strains showed a growth advantage in alkaline medium.

We sought to determine whether the fitness advantage acquired by the evolved strains was pH dependent. The growth of high-pH-evolved isolates was tested at low pH, near the end of the pH range allowing growth of *E. coli* (Fig. 3). The growth rates and culture densities were tested for isolates B11-1, F7-2, D9-1, and G9-1 cultured in potassium-modified Luria broth (LBK) medium buffered with homo-PIPES [homopiperazine-1,4-bis(2-ethanesulfonic acid)] (pH 4.6). All isolates reached lower 16-h culture densities than the ancestor at pH 4.6 (Tukey test, $P < 0.05$). Thus, the mutations selected in the high-pH-evolved populations slightly decreased the relative fitness at low pH. Growth at pH 7.0 (Fig. 3C) showed mixed results; strains D9-1 and B11-1 showed slightly higher growth than W3110, but the other strains showed no difference.

Deletion of *phoB* enhances growth at high pH. Several mutations found in the high-pH-evolved strains suggest the possibility that knockout or altered activity of these genes might enhance fitness at high pH. To test this possibility, deletions of these genes from the Keio collection were transduced into the ancestor W3110 and their growth rates tested at pH 9.1 (Fig. 4). Each deletion strain was tested in five trials of eight replicates each.

High-pH-evolved strain F7-1 showed an IS*1* insertion knockout of *phoB* (Table 2). Strain W3110 *phoB*::*kanR* showed consistently higher growth than did the ancestor

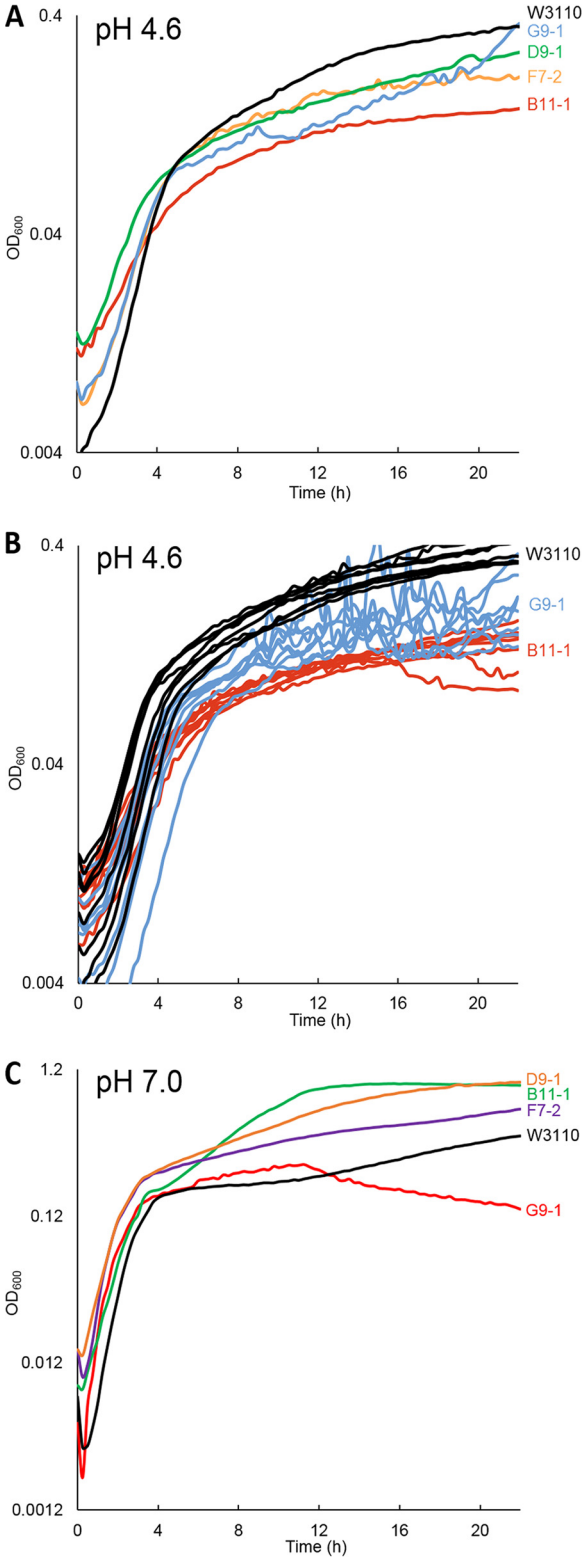

FIG 3 Culture densities for base-evolved strains at pH 4.6 and at pH 7.0. Strains were cultured overnight in LBK medium buffered with MES at pH 5.5 and then diluted 200-fold in medium buffered with homo-PIPES, pH 4.6. All curves shown have median OD_{600} values at 16 h. (A) Strains G9-1, D9-1, G7-2, and B11-1 showed 16-h culture densities significantly higher than that of W3110 (Tukey test, $P < 0.05$). (B) All eight replicates are shown for each strain, G9-1, B11-1, and W3110. (C) Culture densities reached at pH 7.0 in LBK buffered with 100 mM MOPS.

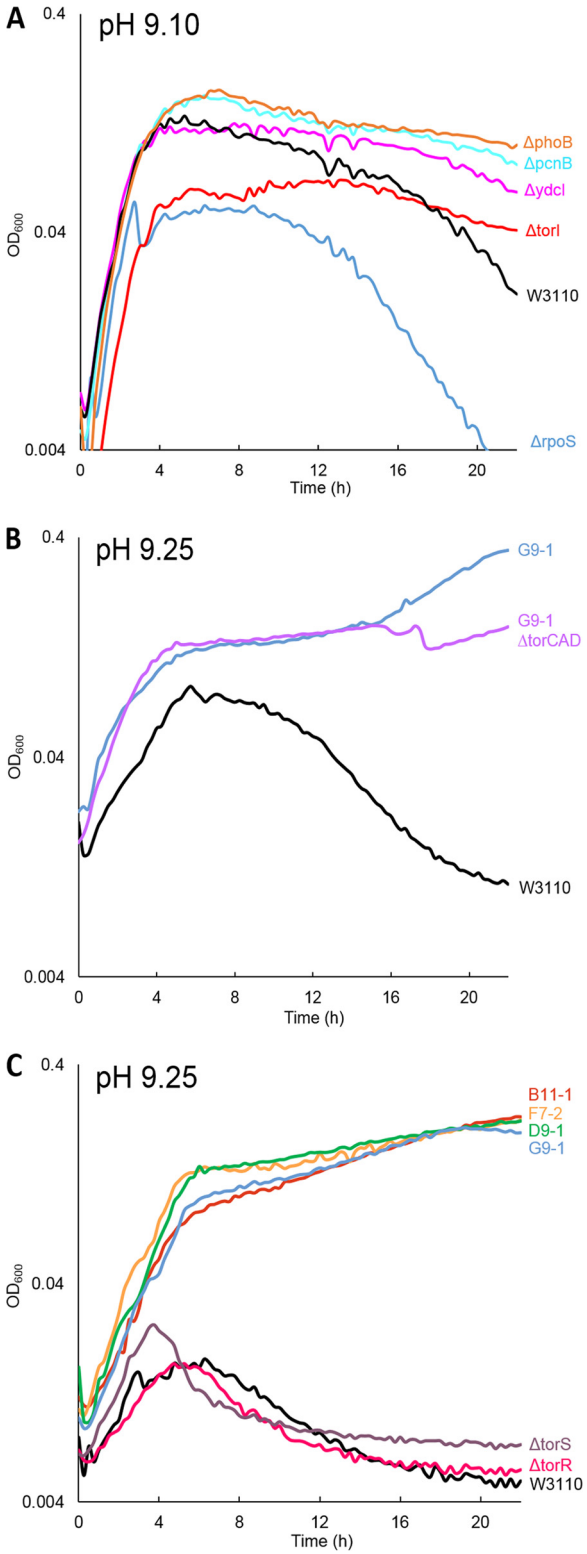

FIG 4 W3110 deletion strains cultured at pH 9.10 or at pH 9.25. Strains were cultured overnight at pH 8.5 as described in Materials and Methods. Overnight cultures were diluted 200-fold into microplate wells with LBK–150 mM AMPSO at pH 9.10; the final pH after 22 h of incubation was 9.1. The curves shown have median OD_{600} values at 16 h. (A) The strains shown are all derivatives of W3110 transduced with Keio deletion Δ*phoB*::*kanR*, Δ*pcnB*::*kanR*, Δ*ydcI*::*kanR*, Δ*torI*::*kanR*, or Δ*rpoS*::*kanR*. Of the deletions tested, the Δ*phoB*::*kanR* and Δ*pcnB*::*kanR* strains showed significantly higher growth at 16 h than strain W3110, whereas the Δ*rpoS*::*kanR* strain showed lower growth (Tukey test, $P < 0.05$). (B) Strain G9-1 with a recombineered Δ*torCAD* deletion showed no significant difference in 16-h culture density compared to

(Continued on next page)

W3110. Thus, *phoB* deletion, with downregulation of the phosphate regulon (8), could be contributing to the high-pH fitness of strain F7-1. The fitness effect of Δ*phoB*, however, was smaller than that seen for F7-2 (Fig. 2A) and was less consistent when tested at pH 9.25. Thus, F7-1 and F7-2 must possess additional mutations contributing to high-pH fitness.

Testing of other high-pH-selected gene deletions. Deletion of other genes showed smaller contributions to high-pH fitness (Fig. 4). The Δ*pcnB*::*kanR* knockout strain outgrew W3110 in 4 out of 6 sets of eight replicates, and the Δ*ydcI*::*kanR* strain outgrew the ancestor in 3 of 6 sets. No fitness effect was seen for deletions Δ*yahO*::*kanR*, Δ*mpl*::*kanR*, Δ*ompT*::*kanR*, Δ*slt*::*kanR*, and Δ*yfcD*::*kanR*. All these genes are likely to have increased fitness during the serial culture of experimental evolution, but revealing their contributions may require extended direct-competition assays (24).

Since three out of four populations showed a deletion including *torI*, we tested whether the loss of *torI* contributes to fitness increase at high pH (Fig. 4A). Strain W3110 Δ*torI*::*kanR* did not grow significantly better than the ancestor. The KplE1 excisionase TorI functions also as a transcriptional regulator of *torCAD*, encoding proteins that reduce trimethylamine *N*-oxide (TMAO), a reaction that may increase pH (20, 22). Since TorI inhibits *torCAD* expression, we hypothesized that deletion of *torI* increases expression of *torCAD* and that *torCAD* expression somehow enhances fitness at high pH. To test this, we recombineered a deletion of *torCAD* in the evolved isolate G9-1. The G9-1 Δ*torCAD* deletion strain was cultured at pH 9.25. W3110 Δ*torCAD* and G9-1 grew almost identically in the pH 9.25 LBK, and both grew significantly better than the ancestor (Fig. 4B) (Tukey test, $P < 0.05$). Thus, *torI* regulation of *torCAD* does not show a fitness effect detectable under the conditions tested. We also tested for a possible fitness contribution of the *torS-torR* phosphorelay system, which mediates TorI inhibition of *torCAD* (20). When cultured at pH 9.25, W3110 Δ*torS*::*kanR* and W3110 Δ*torR*::*kanR* grew as poorly as the W3110 ancestor (Fig. 4C). Similarly, deletion of *torR* from the evolved strain G9-1 showed no significant difference in growth compared to that of the parental strain G9-1 (data not shown).

Mutations in *rpoS*. Mutations affecting RpoS were of interest as they appeared in several high-pH isolates, although none appear to knock out function (Table 2). The *rpoS*-associated mutations found in our evolved strains are point mutations that may have more complex effects on phenotype. In fact, all four populations showed a mutation associated with RpoS, which is necessary for survival at extremely high pH beyond pH 9.8. Both clones in populations F7 and D9 acquired a missense mutation to *rpoS* (E247K) within the open reading frame (ORF). This mutation occurred in region 3 of the RpoS protein, which is responsible for extended −10 promoter recognition (31). Additionally, strain B11 acquired an intergenic mutation (A→G) upstream of *rpoS* in the leader responsible for translational regulation (12). For comparison, a strain containing Δ*rpoS*::*kanR* reached a lower maximum optical density than did the parent W3110 in 4 out of 6 sets of replicates. This result suggests that the mutations found in our experimental evolution do not eliminate RpoS function.

RpoS protein levels and activities vary in the high-pH-evolved strains. We examined the status of RpoS and RpoS activity in the evolved strains, monitoring protein level (Fig. 5A and B) and monitoring RpoS activity by a qualitative measure of catalase activity; the RpoS-dependent *katE* gene encodes catalase HPII (32) (Table 3). RpoS protein levels were examined under two conditions: growth to early exponential phase, when the W3110 parent does not express RpoS (Fig. 5A), and growth to stationary phase, at either pH 7 or pH 9, when W3110 has accumulated RpoS (Fig. 5B). Strains D9 and G9 had significant levels of RpoS in exponential phase, strain B11 had

FIG 4 Legend (Continued)
that of the parent strain G9-1. Both grew significantly more than W3110. (C) Strain W3110 with a deletion of regulator Δ*torR* or of Δ*torS* showed no significant difference in growth compared to that of W3110. All showed lower growth than that of the strains evolved at high pH: B11-1, F7-2, D9-1, and G9-1 (Tukey test, $P < 0.05$).

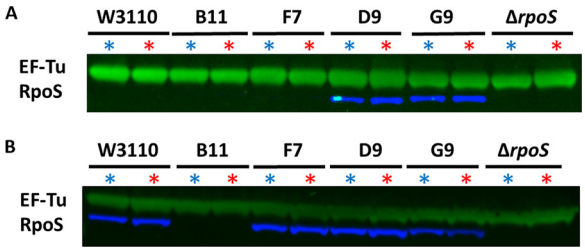

FIG 5 RpoS expression in high-pH-evolved strains. Ancestral strain W3110, evolved isolates (B11-2, F7-1, D9-2, and G9-1), and INH7 (W3110 Δ*rpoS*::*kan*) were grown overnight in LBK buffered with 100 mM MOPS (pH 7.0) at 37°C. Cultures were diluted 1:1,000 into fresh medium (LBK with 100 mM MOPS, pH 7.0) and grown to exponential phase (OD_{600} of 0.1). At an OD_{600} of 0.1, cells were split via filtration into LBK–100 mM MOPS (pH 7.0) or LBK–100 mM TAPS (pH 9.0). (A) Immediately upon the split into pH 7 and pH 9 media, samples were taken and precipitated with 5% trichloroacetic acid (TCA). Samples were analyzed by Western blotting using fluorescent anti-RpoS serum and anti-EF-Tu serum as a loading control. Blue asterisks correspond to samples resuspended in pH 7.0 medium, and red asterisks correspond to samples resuspended in pH 9.0 medium. Note that these strains experience the filtration treatment but have no time to adjust to the changed pH, and thus the two samples can be considered duplicates. (B) Cultures were grown at either pH 7.0 or pH 9.0 for an additional 150 min after the split; these cells were then in stationary phase, where the level of RpoS protein is expected to be high, as seen for W3110. RpoS levels in all evolved isolates are high independent of pH, except for B11, which has barely detectable levels of RpoS at stationary phase.

no visible RpoS under either growth condition, and strain F7 had a pattern similar to that of the W3110 parent. However, all strains had catalase activity less than that of the parent but significantly above that of a Δ*rpoS* derivative of the parent (Table 3). Thus, each of the evolved strains has lowered but not abolished RpoS activity, by different mechanisms.

In strain B11, the leader mutation may decrease translation, consistent with loss of RpoS protein (Fig. 5A and B). In strains F7 and D9, the E247K mutation may decrease RpoS activity. The basis for constitutive expression of RpoS in D9 and G9 was not determined, but possibly the *sspA* mutation in G9-1 contributes to this (Table 2). SspA is a starvation protein that blocks the H-NS repressor, and H-NS in turn represses expression of *iraD* and *iraM* antiadaptors that stabilize RpoS (30, 33). If the *sspA* allele had a gain of function, repressing H-NS more effectively, the resulting expression of the antiadaptors would be expected to increase RpoS accumulation. Given the decreased activity of RpoS in G9-1, we would propose that *sspA* has a loss of function or that one of the other mutations in this lineage is responsible for the decreased activity.

RpoS transcription and translation increase at pH 9.0 compared to pH 7.0. All our high-pH-evolved strains showed decreased but not absent RpoS activity (Table 3), and *rpoS* deletion strains showed pH-sensitive growth (Fig. 4A). Thus, we suspected that high-pH stress, like so many other conditions, might induce RpoS. However, the long-term high RpoS expression might not be optimal for the regrowth after dilution during the evolution experiments. Thus, it could be that these high-pH-evolved populations might show selection for mutations that partly decrease RpoS. We sought to determine if and how RpoS is upregulated during growth at high pH.

RpoS is regulated at multiple levels (12). In addition to transcriptional regulation, translation is inhibited by a hairpin within the 5′ untranslated region (UTR). Under

TABLE 3 Evolved clones exhibit lower RpoS-dependent catalase activity

Strain	O_2 gas formation (0–5)[a]
W3110 Δ*rpoS*::*kan* (INH5)	0
W3110	4.6
B11-2 (JLSH002)	2.3
F7-1 (JLSH003)	3
D9-2 (JLSH006)	2
G9-1 (JLSH007)	2.3

[a]O_2 formation was evaluated qualitatively as described in Materials and Methods; the numbers are the average for three independent observers.

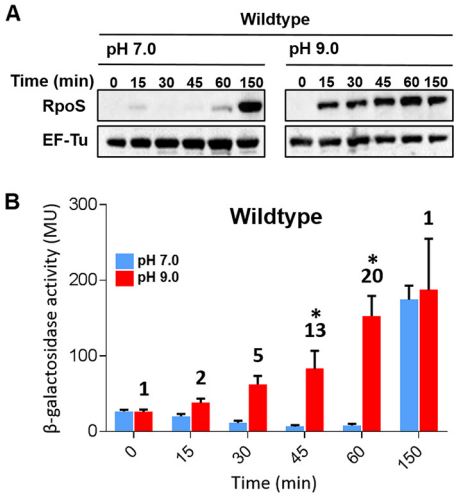

FIG 6 RpoS is induced during growth at pH 9.0. Strain SG30013 expresses wild-type genomic RpoS and also has a *lac* translational fusion to *rpoS*. (A) Bacteria were cultured overnight in LBK–100 mM MOPS (pH 7.0) and then diluted (1:1,000) into fresh medium. Upon growing to an OD_{600} of 0.1, cultures were split via filtration into LBK–100 mM MPOS (pH 7.0) and LBK–100 mM TAPS (pH 9.0). Samples were taken at the time of the initial split and subsequently as indicated. Protein samples were precipitated with 5% TCA and analyzed via Western blotting using an anti-RpoS antiserum. EF-Tu was used as a loading control. (B) Bacteria were cultured as described above. Samples for β-galactosidase activity were prepared and assayed as described by Miller (51) ($n = 3$; error bars = SEM). Blue bars correspond to cultures grown at pH 7.0 and red bars correspond to cultures grown at pH 9.0. Numbers above the bars indicate fold induction at pH 9.0 compared to pH 7.0. Asterisks indicate significant *rpoS* induction at pH 9.0 over pH 7.0 compared to time zero (Tukey test, $P < 0.05$). MU, Miller units.

specific stress conditions, small noncoding RNAs anneal to the 5′ UTR, opening the hairpin and thus activating translation. RpoS protein is degraded, dependent upon the adaptor protein RssB and the ClpXP protease; antiadaptors, induced in response to specific stresses, protect RpoS from degradation.

We first measured RpoS protein accumulation (Fig. 6A) and β-galactosidase activity (Fig. 6B) at pH 9.0 compared to pH 7.0. We used strain SG30013, a derivative of MG1655 that expresses *rpoS* at the wild-type locus in the genome and carries the *rpoS* promoters, leader, and protein fused to a *lacZ* translational reporter gene. This reporter measures all levels of regulation (SG30013) (Table 1). Western blot analysis of RpoS protein accumulation and β-galactosidase activity showed significant upregulation of RpoS at pH 9.0 compared to pH 7.0 within 45 min of exposure at pH 9.0 (Tukey test, $P < 0.05$). At both pH values the cultures showed sustained high-pH induction of RpoS during exponential phase, with a 20-fold increase (pH 9.0 versus pH 7.0) by 60 min (Fig. 6B). In contrast, at pH 7.0 there was no RpoS accumulation until 150 min of growth, when cells had entered stationary phase (Fig. 6B).

Does the high-pH induction of RpoS involve transcriptional regulation? The gene *rpoS* is transcribed primarily from *PrpoS*, initiating within the upstream *nlpD* gene; two *nlpD* promoters also contribute to its expression. To determine if upregulation of transcription contributes to high-pH induction of RpoS, we assayed a transcriptional fusion (NM376) which contains all *rpoS* promoters (*PrpoS*, $PnlpD_1$, and $PnlpD_2$) and 15 nucleotides of the leader fused to *lacZ*. We detected small induction of RpoS within 15 min of exposure to pH 9.0 (Fig. 7A); this contrasts with the 20-fold induction seen after 60 min in Fig. 6. Therefore, only a portion of the response to pH 9.0 is via transcriptional induction. Next, we sought to determine which of the three promoters contribute to the transcriptional induction of RpoS by using an isogenic transcriptional fusion (NM378) containing only one promoter (*PrpoS*). With exposure to an external high pH during exponential phase, we observed a marginal 2-fold induction of RpoS. The positive transcriptional regulation (pH 9.0 versus pH 7.0) at the promoter level comes primarily from *PrpoS* (Fig. 7B, compared to Fig. 7A). Taking the results together, we

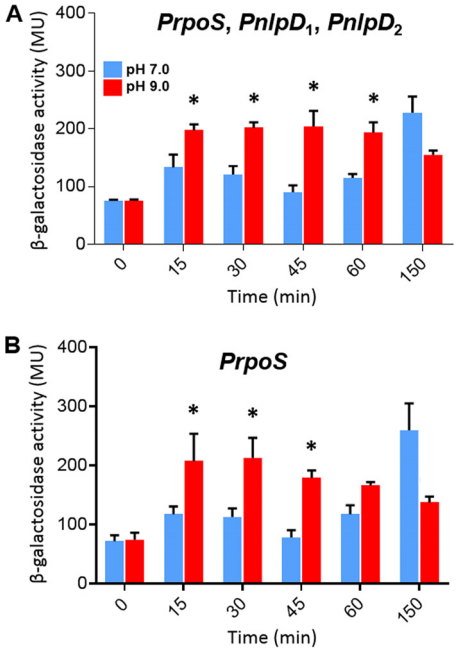

FIG 7 *rpoS* transcription contributes a modest induction at pH 9.0 during exponential growth. (A) Strain NM376 was prepared and assayed for β-galactosidase activity as for Fig. 1. NM376 is a transcriptional fusion that contains all *rpoS* promoters (*Prpo*, *PnlpD*$_1$, and *PnlpD*$_2$) and 15 nucleotides of the leader. (B) Strain NM378 was prepared and assayed for β-galactosidase activity as described for Fig. 1. NM378 possesses only the major *rpoS* promoter (*PrpoS*) and 15 nucleotides of the leader. Blue bars correspond to cultures at pH 7.0 and red bars correspond to cultures at pH 9.0. Asterisks indicate significant *rpoS* induction at pH 9.0 (Tukey test, $P < 0.05$). MU, Miller units.

estimate a 2-fold transcriptional contribution to RpoS induction at pH 9.0 during growth.

We tested the role of regulation at the level of *rpoS* translation. RpoS translation by sRNAs depends on an inhibitory hairpin with the leader. To determine if RpoS translation is upregulated during growth at pH 9.0, we assayed two different translational fusions using the methodology described above (Fig. 8). The first fusion (BA938) contained a constitutive Cp17 prompter, full-length leader, and truncated 477-nucleotide (nt) ORF that lacks the sequence required for RssB-mediated RpoS degradation. The other translational fusion (BA943) was isogenic except for a point mutation (C125T) within the leader. This mutation prevents the formation of the mRNA hairpin loop, thereby leaving the ribosome-binding site (RBS) exposed for RNA polymerase to initiate translation (open hairpin). Both the translational fusions with the wild-type hairpin (BA938) and with the open hairpin (BA943) showed a similar 2-fold induction of RpoS beginning 45 min after exposure to pH 9.0 (Fig. 8A and B). As we saw for transcription, translation of RpoS is modestly increased at pH 9.0. There is no clear evidence of dependence on sRNAs with the hairpin loop (34).

RpoS induction is mediated by antiadaptors IraM, IraP, and IraD. RpoS is rapidly degraded under nonstress conditions, dependent upon adaptor protein RssB, and is stabilized upon expression of three known antiadaptors (IraM, IraP, and IraD) (35). To examine the contribution of protein stabilization to induction at high pH, we first utilized strain SG30018, a derivative of SG30013 carrying a deletion of *rssB* (Table 1). The *rssB* deletion stabilizes RpoS by inhibiting RssB-mediated delivery to the ClpXP protease, thereby mimicking the function of antiadaptor proteins; thus, RpoS should be fully stable in this strain. During growth at pH 9.0, we observe a 4-fold increase of RpoS-LacZ compared to that during growth at pH 7.0 (Fig. 9A). This increase is less than the 20-fold induction seen after 60 min in an *rssB*$^+$ strain (Fig. 6B). This result implies that one or a combination of the known antiadaptors (IraM, IraP, and IraD) or not-yet-identified antiadaptors interacts with adaptor protein RssB to stabilize RpoS at pH 9.0.

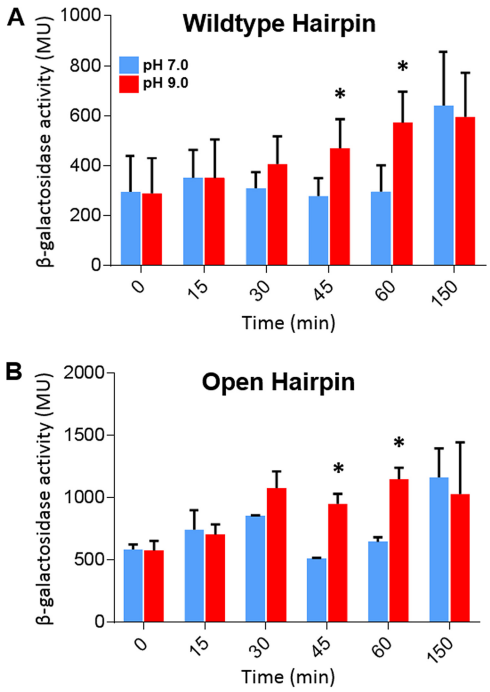

FIG 8 RpoS translation increases modestly beginning after 30 min in an mRNA hairpin-independent manner. (A) Strain BA938 was prepared and assayed for β-galactosidase activity as described for Fig. 1. BA938 is an *rpoS-lacZ* translational fusion constitutively expressed by a Cp17 promoter. Additionally, BA938 has a truncated *rpoS* ORF (477 nt) which lacks the region necessary for RssB-dependent degradation. (B) Strain BA943 was prepared and assayed for β-galactosidase activity as for Fig. 1. BA943 is a derivative of BA938 with a C125T mutation, which prevents the formation of the *rpoS* mRNA hairpin loop, thereby preventing occlusion of the RBS. Asterisks indicate significant *rpoS* induction at pH 9.0 (Tukey test, $P < 0.05$). MU, Miller units.

A derivative of SG30013 that was mutant for all three antiadaptors, *iraM*, *iraP*, and *iraD* (INH5), was grown and assayed as before in buffered alkaline medium (pH 9.0) (Fig. 9B). This strain had a lower level of expression of the fusion protein, consistent with loss of antiadaptor-mediated stabilization, and showed no RpoS induction at pH 9.0 compared to pH 7.0.

Overall, our results demonstrate significant induction of RpoS upon exposure to pH 9.0. Stabilization of the protein, at least in part due to one or more of the known antiadaptors, contributes around 5-fold to induction; transcription and translation each contribute about 2-fold, for an overall induction, after 60 min, of 20-fold. Thus, high-pH treatment has multiple effects on the RpoS sensing pathway.

To confirm that pH 9.0 did not affect the constitutive Cp17 promoter or *lacZ* fusion, we assayed a control strain that had a Cp17::*lacZ* fusion in an SG30013 background at pH 7.0 and pH 9.0. When grown at pH 7.0 or pH 9.0, RpoS was induced equally with little variation (Fig. 10). This result indicates that pH 9.0 does not affect the expression of Cp17 or *lacZ*.

DISCUSSION

Experimental evolution of *E. coli* at pH 9.0 to 9.3 yielded strains that grow at pH values significantly higher than that for the ancestral strain. Genomic analysis of eight isolates revealed approximately 50 mutations that may be contributing to fitness at pH 9.0. As found in our previous pH stress evolution experiments, many of the mutations involved knockout of regulators (25, 27). The knockout of acid-inducible *phoB* shows a clear contribution to high-pH fitness, which could be associated with the increased production of fermentation acids.

Three out of four populations (F7, D9, and G9) acquired a deletion of the KPlE1 prophage, which carries *torI*, a transcriptional activator of the *torCAD* operon. Induction

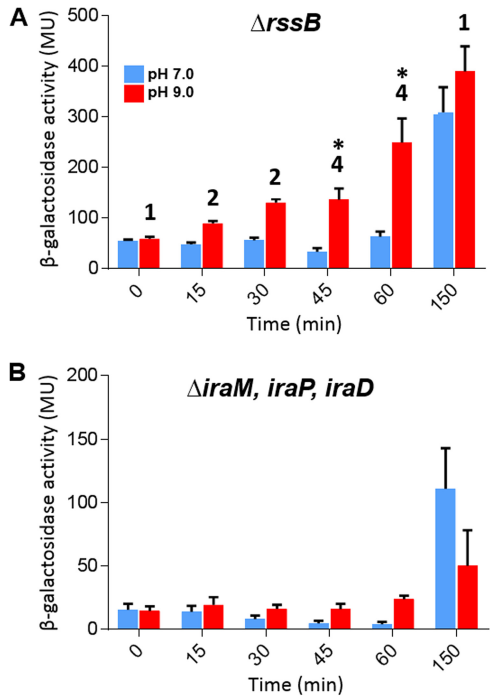

FIG 9 RpoS stability contributes a 4-fold induction of RpoS expression during growth at pH 9.0, likely through known antiadaptors IraD, IraM, and IraP. (A) A Δ*rssB* mutant (SG30018, with stabilized RpoS) was prepared and assayed for β-galactosidase activity as for Fig. 1. (B) A Δ*iraM* Δ*iraP* Δ*iraD* mutant (INH5) was grown and assayed for β-galactosidase activity as described for Fig. 1 ($n = 3$; error bars = SEM). Asterisks indicate significant *rpoS* promoter induction at pH 9.0 (Tukey test, $P < 0.05$). MU, Miller units.

of *torCAD* downregulates known acid resistance genes *gadA*, *gadBC*, *hdeAB*, *hdeD*, *yhiE*, and *yhiM* and positively regulates base resistance genes *tnaLAB*, possibly in anticipation of alkalization of the medium caused by TMAO reduction to trimethylamine (20). Deletion of *torCAD* did not appear to decrease the fitness of strain G9-1 under the conditions tested (one daily dilution cycle), but given the appearance of the deletion in multiple populations, it is likely that *torCAD* expression has a fitness contribution that could be demonstrated by more sensitive means such as a multicycle direct competition. For the future, our lab is establishing a sensitive fluorescence-activated cell sorting (FACS) system for competition analysis (36).

The high-pH-evolved isolates showed a striking pattern of point mutations in the RpoS stress sigma factor, whose fitness contributions remain unclear. RpoS is required for survival at extremely high pH (pH 9.8) (15), and it mediates regulation of base resistance proteins (10, 13). This connection may be related to the fact that the pH rises during culture growth to stationary phase in unbuffered tryptone-yeast extract medium

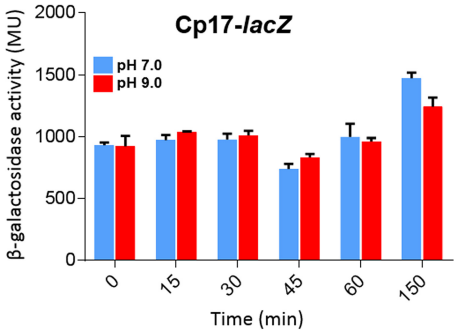

FIG 10 pH 9.0 does not affect the stability or activity of the Cp17 constitutive promoter or the *lacZ* gene. Strain BA926 is a derivative of MG1655 with a Cp17-*lacZ* transcriptional fusion. MU, Miller units.

(37, 38). Our subculturing cycle subjected bacteria to repeated periods of stationary phase, conditions under which *rpoS* mutations accumulate as part of the "growth advantage in stationary phase" (GASP) response (39, 40). Multiple rounds of stationary phase, with concomitant high pH, also lead to mutations in the *rpoS* activator *sspA* (41), which showed a mutant allele in one of our base-evolved populations (population G9).

One possible explanation for the selection of *rpoS* variant alleles in our populations is that the short-term benefits of RpoS at high pH have an associated cost under long-term exposure. A comparable short-term and long-term trade-off is seen for the acid-inducible amino acid decarboxylases at low pH (27). Consistent with this role, we found that RpoS is induced during growth at pH 9.0 but not at pH 7.0. This upregulation of RpoS allows expression of proteins needed for nongrowth survival at extremely high pH (pH >9.8). Analysis of *rpoS-lacZ* fusions revealed a complex pathway for induction. Transcriptional fusions showed a 2-fold contribution to RpoS induction primarily from *PrpoS* (Fig. 7). Similarly, translational fusions revealed a 2-fold induction. The regulatory details we observed must be qualified by the fact that different media and strains were used for the molecular experiments and the evolution experiments.

Under certain stresses, RpoS translation is positively regulated with the help of chaperone protein Hfq via direct binding of small regulatory RNAs (sRNAs) to the RpoS mRNA hairpin (42). When an sRNA binds to an mRNA hairpin, the hairpin is opened and the ribosome may bind to the RBS to initiate translation (17). However, we saw no clear evidence that RpoS induction is affected by the opening of the sRNA hairpin loop (Fig. 8). It is unclear what may be causing transcriptional or translational RpoS induction.

In our experiments, the greatest contribution to RpoS induction came from protein stabilization, via inhibition of RssB-mediated ClpXP proteolysis of RpoS (Fig. 9). At least one of the three characterized antiadaptors (*iraM*, *iraP*, and *iraD*) clearly contributes to this stabilization, but it may not account for all of it (Fig. 9B). It would be interesting to determine which of the three antiadaptors may be stabilizing RpoS and how high pH induces this response. IraP and IraD are known to be induced in response to the alarmone ppGpp (43, 44); if high pH increases ppGpp (44), we would predict that these antiadaptors will be critical for high-pH induction. Elevated ppGpp levels might also explain the minor transcriptional induction.

Our investigation of the expression of RpoS protein levels and RpoS activity in the evolved strains demonstrates that they have all taken different pathways to the same final phenotype, that is, RpoS activity levels that are lower than those of the wild-type strain but significantly above those of a strain devoid of RpoS. This proposed mechanism is consistent with the combination of a need for RpoS to cope with the perpetual high-pH stress coupled with compensation for some fitness cost of the high RpoS levels resulting from high pH. The evolution to reduced but not absent RpoS is strikingly similar to the case for *rpoS* alleles isolated as advantageous for long-term stationary-phase growth (45), reinforcing the importance of having enough but not too much RpoS.

MATERIALS AND METHODS

Strains and culture media. The strains used in this study are listed in Table 1. All high-pH-evolved isolates were derived from a W3110 K-12 ancestor (lab stock D-8; originally from F. Neidhardt) (24). For RpoS induction experiments, strains were constructed starting with SG30013. SG30013 is a derivative of MG1655 containing a translational fusion of *lacZ* fused to the promoters, leader, and first 250 amino acids of the *rpoS* gene (46).

Bacteria were cultured at 37°C in Luria broth supplemented with potassium (LBK) (10 g/liter tryptone, 5 g/liter yeast extract, 7.45 g/liter KCl). The medium was buffered with either 100 mM 2-(*N*-morpholino) ethanesulfonic acid (MES) (pK_a = 5.96), 100 mM 3-(*N*-morpholino)propane-1-sulfonic acid (MOPS) (pK_a = 7.20), [(2-hydroxy-1,1-bis(hydroxymethyl)ethyl)amino]-1-propanesulfonic acid (TAPS) (pK_a = 8.4), or *N*-(1,1-dimethyl-2-hydroxyethyl)-3-amino-2-hydroxypropanesulfonic acid (AMPSO); pKa = 9.0). The pH was adjusted accordingly using 5 M KOH. All cultures were incubated at 37°C unless stated otherwise.

High-pH (pH 9.25) experimental evolution. High-pH experimental evolution was modeled after our previous laboratory evolution experiments conducted in the presence of external acid and permeant acid (24, 25). Twenty-four high-pH-evolved populations originated from the same K-12 W3110 (lab stock, D-8) ancestor. The ancestral strain was cultured overnight in LBK with 100 mM TAPS (pH 8.5) and then diluted (1:200) into 24 wells containing 200 μl LBK with 150 mM TAPS (pH 9.0). The plate was then

incubated in a SpectraMax Plus384 MicroPlate reader (Molecular Devices) at 37°C for 22 h while optical density at 45 nm (OD_{450}) readings were recorded every 15 min after shaking for 3 s. After 22 h, the cultures were diluted (1:100) into fresh medium in a new 96-well plate and grown identically. The old plates were stored at −80°C with addition of 100 μl 50% glycerol–100 mM MOPS (pH 7.5) to each well population. Diluting the evolving cultures 1:100 resulted in approximately 6.6 generations per day. If a culture did not grow, the experiment was restarted by taking a 1:50 dilution from the most recent frozen plate into fresh medium. All populations underwent the same number of generations.

The cells were initially subcultured in LBK with 150 mM TAPS (pH 9.0) and serially subcultured for an estimated 470 generations, at which point the buffer was changed to 150 mM AMPSO to better accommodate an increase in the pH of the medium to 9.2. Cells were subcultured at pH 9.2 for an additional 730 generations; then, at generation 1,200, the pH was increased to 9.25, and at generation 1,900 the pH was increased to 9.3. The experiment was terminated after 2,200 generations, and isolates were obtained for genome sequencing.

Whole-genome sequencing. The genomes of eight evolved strains and of the ancestral strain W3110 were resequenced (Table 1). The DNA from each strain was extracted using a DNeasy kit (Qiagen). Sequencing was performed by the Research and Technology Support Facility at Michigan State University. Libraries were prepared using the Illumina TruSeq Nano DNA library preparation kit. Illumina MiSeq 2 × 250 base calling was performed by Illumina Real Time Analysis (RTA) v1.18.54, and the output of RTA was demultiplexed and converted to Fastq format with Illumina Bcl2fastq v1.8.4. The number of reads for each of 8 genomes ranged from 900,000 to 1,900,000. Average quality scores ranged from Q30 to Q36.

Genome sequences were aligned to the reference *E. coli* K-12 W3110 (GenBank accession number NC_007779.1), and mutations were predicted using the breseq 0.30.0 computational pipeline (23, 47). Unassigned alignment variants were inspected for deletions and insertions.

Strain construction. P1 phage transduction was conducted to construct deletion strains with *kanR* insertions (24) using *kanR* replacement strains obtained from the Keio collection (Coli Genetic Stock Center, Yale University) (48).

A Δ*torCAD* deletion was constructed by recombineering (49, 50). The counterselectable *cat-sacB* cassette was PCR amplified from colonies of *E. coli* strain XLT241 using primers that have 5′ homology to the flanking regions of *torCAD* (5′-TGTTCATATTTGCTCATTAAGATCGCTTCACTAAACCATAATTCTATGTG ACGGAAGATCACTTCGCA-3′ and 5′-ATGCCTGATGCGACGCTAAACGCGTCTTTTCAGGCGCACAAACATCAAA GGGAAAACTGTCCATATGCA-3′). High-pH-evolved isolate G9-1 transformed with the heat-inducible pSIM6::*ampR* plasmid was cultured to mid-log phase at 32°C and then transferred to 42°C to induce recombineering proteins. Cells were made electrocompetent and electroporated with the PCR product of *cat-sacB* containing flanking homology to *torCAD*. The transformed cells were outgrown at 32°C for 3 to 5 h and plated on LB containing 10 μg/ml chloramphenicol. Successful colonies were screened for resistance to chloramphenicol and sensitivity to sucrose. To remove the *cat-sacB* cassette, the successful colonies were made electrocompetent, electroporated with a DNA oligonucleotide with flanking homology to *torCAD* (5′-TGCTCATTAAGATCGCTTCACTAAACCATAATTCTAGTTTGTGCGCCTGAAAAGACGCGTTTA GCGTCGCA-3′), and then plated on LB agar plates lacking NaCl but containing 6% sucrose. Successful colonies were further screened for resistance to sucrose and sensitivity to chloramphenicol. The *torCAD* deletion was then confirmed by PCR sequencing (with 5′-CTGTTCATATTCTGCCGTAAGC-3′ and 5′-GTG TTTGCCGGATGCGATGA-3′).

Strains NM376 and 378 were constructed by recombineering a 3-way PCR product into strain NM1100 (35). In a first step, PCR was used to amplify a zeocin cassette with a 5′-end 40-nt homology to the end of *lacI*, using oligonucleotides lacI-Zeo_inv.F1 (GCTGGCACGACAGGTTTCCCGACTGGAAAGCGGG CAGTGAAAAAAAAGCCCGCTCATTAG) and zeo-rpoS_inv.R1 (GCAAAATAACCAGGAAAAATCCAGGTATTTC CTCACGTTTGTTGACAATTAATCATCGGC). In parallel, a second PCR product was created carrying the *rpoS* fragment that has 40 nt of homology at its 5′ end to the 3′ end of the zeocin cassette and 40 nt of homology to the +1 of *lacZ* at the 3′ end, using oligonucleotides Zeo-rpoS_inv.F2 (GCCGATGATTAATT GTCAACAAACGTGAGGAAATACCTGG) and either rpoS-lacZ.R2a for NM376 (ATAGCTGTTTCCTGTGTGAAA TTGTTATCCGCTCACAATTACTCTGTTCACCCGAAGACT) or rpoS-lacZ.R2b for NM378 (ATAGCTGTTTCCTGT GTGAAATTGTTATCCGCTCACAATTGCTCGGTTGTGCTTGCTGTT). The two PCR primers were then mixed together into a third PCR mixture, using flanking primers (lacI-Zeo inv.F1 with either rpoS-lacZ.R2a or rpoS-lacZ.R2b) to create one fragment carrying both the zeocin cassette and appropriate *rpoS* fragment. This final PCR product was then used in a recombineering reaction into NM1100 as described elsewhere (35), selecting for clones growing on LB-zeocin plates. All constructs were checked by sequencing.

Measurement of high-pH growth. The eight evolved strains (B11-1, B11-2, D9-1, D9-2, F7-1, F7-2, G9-1, and G9-2) (Table 1), the ancestral strain (W3110), and the transduced strains were cultured in LBK and buffered with 100 mM TAPS at a pH of 8.5 for 16 to 18 h at 37°C with shaking. Initial overnight growth with a milder stress increases the consistency of quality of the overnight culture, which varies depending on the size of the colony picked. The cultures were diluted into LBK buffered with 150 mM AMPSO at pH 9.25 at a 1:200 concentration in a 96-well plate, with eight replicate wells for each strain. Plates were incubated in the SpectraMax Plus384 MicroPlate reader (Molecular Devices) for 22 h at 37°C. The OD_{600} was measured every 15 min with shaking for 3 s before reads, and data were compiled using Softmax Pro version 6.4.2. Endpoint density was measured at 600 nm after 16 h. The pH of the culture medium was measured before and after growth. The final pH was measured by combining the solutions of the eight replicate wells for each strain. pH measurements were performed at room temperature. The change in pH during growth was <0.2 unit.

The rate of doublings per hour (*k*) was calculated during logarithmic growth phase. For each strain, eight replicates were tested from independent overnight cultures. For statistical analysis, analysis of

variance (ANOVA) and Tukey honestly significant difference (HSD) tests were conducted on the log-phase growth rates and on the $\log_2$ values of the 16-h culture densities.

***β*-Galactosidase assay for RpoS induction.** Overnight cultures were incubated for 16 to 18 h in LBK with 100 mM MOPS (pH 7.0) and then diluted (1:1,000) into fresh medium to minimize residual levels of stationary-phase RpoS. Upon reaching an OD_{600} of 0.1, each culture was split via filtration and suspended into equal 30-ml volumes of LBK–100 mM MOPS (pH 7.0) and LBK–100 mM TAPS (pH 9.0). Samples were taken at the time of initial exposure and subsequently at timed intervals during aerated growth in a rotating water bath set to 37°C. Samples were assayed, and enzyme activity was measured (51). For statistical analysis, ANOVA and Tukey HSD tests were conducted on the ratios of enzyme activity (pH 9.0 versus pH 7.0) from three independent trials for the assay times presented.

Western blotting for RpoS induction. Strains were cultured under conditions identical to those for the β-galactosidase assay for RpoS induction, and samples for both assays were taken simultaneously (see above). Cells were precipitated with trichloroacetic acid (5% total volume) and washed with 80% acetone. Samples were suspended in SDS loading buffer (Invitrogen) and normalized according to the OD_{600}. Samples were isolated using a 12% Bis-Tris gel (Invitrogen) and transferred onto a nitrocellulose membrane (Invitrogen). Membranes were probed with a 1:5,000 dilution of anti-RpoS antibody, and loading was normalized to an EF-Tu control. Images were obtained with a ChemiDoc MP imaging system (Bio-Rad).

Catalase assay of RpoS activity. Strains were streaked on LB plates and incubated overnight at 37°C, and a colony was picked from a plate and submerged into 1 ml of 3% H_2O_2 without mixing. Bubbles (O_2 formation) were immediately evaluated on a scale of 0 (none) to 5 (wild-type strain) by an observer who was not told the identity of the strains; three independent trials were done, using different colonies and different observers for each, and their ratings were averaged. The method was as described at http://learn.chm.msu.edu/vibl/content/catalase.html.

Accession number(s). Sequence data have been deposited in the NCBI Sequence Read Archive (SRA) under accession number SRP074502.

ACKNOWLEDGMENTS

This work was funded by National Science Foundation grant MCB1613278 and in part by the Intramural Research Program of the NIH, National Cancer Institute, Center for Cancer Research.

We thank Lynn Thomason and Jeremy Moore for the gift of strains and instruction in recombineering. We thank Francois De Mets and Thomas Delerue for providing the evaluation of the levels of catalase in the evolved strains.

REFERENCES

1. Foster JW. 2004. *Escherichia coli* acid resistance: tales of an amateur acidophile. Nat Rev Microbiol 2:898–907. https://doi.org/10.1038/nrmicro1021.
2. Padan E, Bibi E, Ito M, Krulwich TA. 2005. Alkaline pH homeostasis in bacteria: new insights. Biochim Biophys Acta Biomembr 1717:67–88. https://doi.org/10.1016/j.bbamem.2005.09.010.
3. Wilks JC, Slonczewski JL. 2007. pH of the cytoplasm and periplasm of *Escherichia coli*: rapid measurement by green fluorescent protein fluorimetry. J Bacteriol 189:5601–5607. https://doi.org/10.1128/JB.00615-07.
4. Slonczewski JL, Rosen BP, Alger JR, Macnab RM. 1981. pH homeostasis in *Escherichia coli*: measurement by P^{31} nuclear magnetic resonance of methylphosphonate and phosphate. Proc Natl Acad Sci U S A 78:6271–6275.
5. Blankenhorn D, Phillips J, Slonczewski JL. 1999. Acid- and base-induced proteins during aerobic and anaerobic growth of *Escherichia coli* revealed by two-dimensional gel electrophoresis. J Bacteriol 181:2209–2216.
6. Maurer LM, Yohannes E, Bondurant SS, Radmacher M, Slonczewski JL. 2005. pH regulates genes for flagellar motility, catabolism, and oxidative stress in *Escherichia coli* K-12. J Bacteriol 187:304–319. https://doi.org/10.1128/JB.187.1.304-319.2005.
7. Hayes ET, Wilks JC, Sanfilippo P, Yohannes E, Tate DP, Jones BD, Radmacher MD, BonDurant SS, Slonczewski JL. 2006. Oxygen limitation modulates pH regulation of catabolism and hydrogenases, multidrug transporters, and envelope composition in *Escherichia coli* K-12. BMC Microbiol 6:89. https://doi.org/10.1186/1471-2180-6-89.
8. Marzan LW, Shimizu K. 2011. Metabolic regulation of *Escherichia coli* and its *phoB* and *phoR* genes knockout mutants under phosphate and nitrogen limitations as well as at acidic condition. Microb Cell Fact 10:39. https://doi.org/10.1186/1475-2859-10-39.
9. Marzan LW, Hasan CMM, Shimizu K. 2013. Effect of acidic condition on the metabolic regulation of *Escherichia coli* and its *phoB* mutant. Arch Microbiol 195:161–171. https://doi.org/10.1007/s00203-012-0861-7.
10. Dover N, Padan E. 2001. Transcription of *nhaA*, the main Na^+/H^+ antiporter of *Escherichia coli*, is regulated by Na^+ and growth phase. J Bacteriol 183:644–653. https://doi.org/10.1128/JB.183.2.644-653.2001.
11. Huang Y, Chen W, Dotson DL, Beckstein O, Shen J. 2016. Mechanism of pH-dependent activation of the sodium-proton antiporter NhaA. Nat Commun 7:12940. https://doi.org/10.1038/ncomms12940.
12. Battesti A, Majdalani N, Gottesman S. 2011. The RpoS-mediated general stress response in *Escherichia coli*. Annu Rev Microbiol 65:189–213. https://doi.org/10.1146/annurev-micro-090110-102946.
13. Wong GT, Bonocora RP, Schep AN, Beeler SM, Fong AJL, Shull LM, Batachari LE, Dillon M, Evans C, Becker CJ, Bush EC, Hardin J, Wade JT, Stoebel DM. 2017. Genome-wide transcriptional response to varying RpoS levels in *Escherichia coli* K-12. J Bacteriol 199:755–816. https://doi.org/10.1128/JB.00755-16.
14. Mandel MJ, Silhavy TJ. 2005. Starvation for different nutrients in *Escherichia coli* results in differential modulation of RpoS levels and stability. J Bacteriol 187:434–442. https://doi.org/10.1128/JB.187.2.434-442.2005.
15. Small P, Blankenhorn D, Welty D, Zinser E, Slonczewski JL. 1994. Acid and base resistance in *Escherichia coli* and *Shigella flexneri*: role of *rpoS* and growth pH. J Bacteriol 176:1729–1737. https://doi.org/10.1128/jb.176.6.1729-1737.1994.
16. Lange R, Hengge-Aronis R. 1994. The cellular concentration of the σS subunit of RNA polymerase in *Escherichia coli* is controlled at the levels of transcription, translation, and protein stability. Genes Dev 8:1600–1612. https://doi.org/10.1101/gad.8.13.1600.
17. Storz G, Vogel J, Wassarman KM. 2011. Regulation by small RNAs in bacteria: expanding frontiers. Mol Cell 43:880–891. https://doi.org/10.1016/j.molcel.2011.08.022.
18. Schweder T, Lee KHO, Lomovskaya O, Matin A. 1996. Regulation of

Escherichia coli starvation sigma factor (σs) by ClpXP protease. J Bacteriol 178:470–476. https://doi.org/10.1128/jb.178.2.470-476.1996.
19. Battesti A, Hoskins JR, Tong S, Milanesio P, Mann JM, Kravats A, Tsegaye YM, Bougdour A, Wickner S, Gottesman S. 2013. Anti-adaptors provide multiple modes for regulation of the RssB adaptor protein. Genes Dev 27:2722–2735. https://doi.org/10.1101/gad.229617.113.
20. Bordi C, Théraulaz L, Méjean V, Jourlin-Castelli C. 2003. Anticipating an alkaline stress through the Tor phosphorelay system in *Escherichia coli*. Mol Microbiol 48:211–223. https://doi.org/10.1046/j.1365-2958.2003.03428.x.
21. Barrett EL, Kwan HS. 1985. Bacterial reduction of trimethylamine oxide. Annu Rev Microbiol 39:131–149. https://doi.org/10.1146/annurev.mi.39.100185.001023.
22. Ansaldi M, Théraulaz L, Mejean V. 2004. TorI, a response regulator inhibitor of phage origin in *Escherichia coli*. Proc Natl Acad Sci U S A 101:9423–9428. https://doi.org/10.1073/pnas.0401927101.
23. Deatherage DE, Barrick JE. 2014. Identification of mutations in laboratory-evolved microbes from next-generation sequencing data using breseq. Methods Mol Biol 1151:165–188. https://doi.org/10.1007/978-1-4939-0554-6_12.
24. Harden MM, He A, Creamer K, Clark MW, Hamdallah I, Martinez KA, Kresslein RL, Bush SP, Slonczewski JL. 2015. Acid-adapted strains of *Escherichia coli* K-12 obtained by experimental evolution. Appl Environ Microbiol 81:1932–1941. https://doi.org/10.1128/AEM.03494-14.
25. Creamer KE, Ditmars FS, Basting PJ, Kunka KS, Hamdallah IN, Bush SP, Scott Z, He A, Penix SR, Gonzales AS, Eder EK, Camperchioli DW, Berndt A, Clark MW, Rouhier KA, Slonczewski JL. 2017. Benzoate- and salicylate-tolerant strains of *Escherichia coli* K-12 lose antibiotic resistance during laboratory evolution. Appl Environ Microbiol 83:2736–2816. https://doi.org/10.1128/AEM.02736-16.
26. Blount ZD, Borland CZ, Lenski RE. 2008. Historical contingency and the evolution of a key innovation in an experimental population of *Escherichia coli*. Proc Natl Acad Sci U S A 105:7899–7906. https://doi.org/10.1073/pnas.0803151105.
27. He A, Penix SR, Basting PJ, Griffith JM, Creamer KE, Camperchioli D, Clark MW, Gonzales AS, Sebastian Chávez Erazo J, George NS, Bhagwat AA, Slonczewski JL. 2017. Acid evolution of *Escherichia coli* K-12 eliminates amino acid decarboxylases and reregulates catabolism. Appl Environ Microbiol 83:442–517. https://doi.org/10.1128/AEM.00442-17.
28. Casjens S. 2003. Prophages and bacterial genomics: what have we learned so far? Mol Microbiol 49:277–300. https://doi.org/10.1046/j.1365-2958.2003.03580.x.
29. ElAntak L, Ansaldi M, Guerlesquin F, Méjean V, Morelli X. 2005. Structural and genetic analyses reveal a key role in prophage excision for the TorI response regulator inhibitor. J Biol Chem 280:36802–36808. https://doi.org/10.1074/jbc.M507409200.
30. Hansen AM, Qiu Y, Yeh N, Blattner FR, Durfee T, Jin DJ. 2005. SspA is required for acid resistance in stationary phase by downregulation of H-NS in *Escherichia coli*. Mol Microbiol 56:719–734. https://doi.org/10.1111/j.1365-2958.2005.04567.x.
31. Campbell EA, Muzzin O, Chlenov M, Sun JL, Olson CA, Weinman O, Trester-Zedlitz ML, Darst SA. 2002. Structure of the bacterial RNA polymerase promoter specificity σ subunit. Mol Cell 9:527–539. https://doi.org/10.1016/S1097-2765(02)00470-7.
32. Schellhorn HE, Stones VL. 1992. Regulation of *katF* and *katE* in *Escherichia coli* K-12 by weak acids. J Bacteriol 174:4769–4776. https://doi.org/10.1128/jb.174.14.4769-4776.1992.
33. Dalebroux ZD, Swanson MS. 2012. ppGpp: magic beyond RNA polymerase. Nat Rev Microbiol 10:203–212. https://doi.org/10.1038/nrmicro2720.
34. Battesti A, Majdalani N, Gottesman S. 2015. Stress sigma factor RpoS degradation and translation are sensitive to the state of central metabolism. Proc Natl Acad Sci U S A 112:5159–5164. https://doi.org/10.1073/pnas.1504639112.
35. Bougdour A, Cunning C, Baptiste PJ, Elliott T, Gottesman S. 2008. Multiple pathways for regulation of σS (RpoS) stability in *Escherichia coli* via the action of multiple anti-adaptors. Mol Microbiol 68:298–313. https://doi.org/10.1111/j.1365-2958.2008.06146.x.
36. Gullberg E, Cao S, Berg OG, Ilbäck C, Sandegren L, Hughes D, Andersson DI. 2011. Selection of resistant bacteria at very low antibiotic concentrations. PLoS Pathog 7:e1002158. https://doi.org/10.1371/journal.ppat.1002158.
37. Stancik LM, Stancik DM, Schmidt B, Barnhart DM, Yoncheva YN, Slonczewski JL. 2002. pH-dependent expression of periplasmic proteins and amino acid catabolism in *Escherichia coli*. J Bacteriol 184:4246–4258. https://doi.org/10.1128/JB.184.15.4246-4258.2002.
38. Kram KE, Finkel SE. 2014. Culture volume and vessel affect long-term survival, mutation frequency, and oxidative stress of *Escherichia coli*. Appl Environ Microbiol 80:1732–1738. https://doi.org/10.1128/AEM.03150-13.
39. Zinser ER, Kolter R. 2000. Prolonged stationary-phase incubation selects for *lrp* mutations in *Escherichia coli* K-12. J Bacteriol 182:4361–4365. https://doi.org/10.1128/JB.182.15.4361-4365.2000.
40. Chib S, Ali F, Seshasayee ASN. 2017. Genomewide mutational diversity in Escherichia coli population evolving in prolonged stationary phase. mSphere 2:e00059-17. https://doi.org/10.1128/mSphere.00059-17.
41. Kram KE, Geiger C, Ismail WM, Lee H, Tang H, Foster PL, Finkel SE. 2017. Adaptation of Escherichia coli to long-term serial passage in complex medium: evidence of parallel evolution. mSystems 2:e00192-16. https://doi.org/10.1128/mSystems.00192-16.
42. Brennan RG, Link TM. 2007. Hfq structure, function and ligand binding. Curr Opin Microbiol 10:125–133. https://doi.org/10.1016/j.mib.2007.03.015.
43. Merrikh H, Ferrazzoli AE, Bougdour A, Olivier-Mason A, Lovett ST. 2009. A DNA damage response in *Escherichia coli* involving the alternative sigma factor, RpoS. Proc Natl Acad Sci U S A 106:611–616. https://doi.org/10.1073/pnas.0803665106.
44. Bougdour A, Gottesman S. 2007. ppGpp regulation of RpoS degradation via anti-adaptor protein IraP. Proc Natl Acad Sci U S A 104:12896–12901. https://doi.org/10.1073/pnas.0705561104.
45. Zambrano MM, Siegele DA, Almiron M, Tormo A, Kolter R. 1993. Microbial competition: *Escherichia coli* mutants that take over stationary phase cultures. Science 259:1757–1760. https://doi.org/10.1126/science.7681219.
46. Wassarman KM, Repoila F, Rosenow C, Storz G, Gottesman S. 2001. Identification of novel small RNAs using comparative genomics and microarrays. Genes Dev 15:1637–1651. https://doi.org/10.1101/gad.901001.
47. Deatherage DE, Traverse CC, Wolf LN, Barrick JE. 2015. Detecting rare structural variation in evolving microbial populations from new sequence junctions using breseq. Front Genet 5:468. https://doi.org/10.3389/fgene.2014.00468.
48. Baba T, Ara T, Hasegawa M, Takai Y, Okumura Y, Baba M, Datsenko KA, Tomita M, Wanner BL, Mori H. 2006. Construction of *Escherichia coli* K-12 in-frame, single-gene knockout mutants: the Keio collection. Mol Syst Biol 2:2006.0008. https://doi.org/10.1038/msb4100050.
49. Sharan SK, Thomason LC, Kuznetsov SG, Court DL. 2009. Recombineering: a homologous recombination-based method of genetic engineering. Nat Protoc 4:206–223. https://doi.org/10.1038/nprot.2008.227.
50. Thomason LC, Sawitzke JA, Li X, Costantino N, Court DL. 2014. Recombineering: genetic engineering in bacteria using homologous recombination. Curr Protoc Mol Biol 106:1.16.1–1.16.39. https://doi.org/10.1002/0471142727.mb0116s106.
51. Miller JH. 1992. A short course in bacterial genetics: a laboratory manual and handbook for *Escherichia coli* and related bacteria. Cold Spring Harbor Laboratory Press, Cold Spring Harbor, NY.
52. Zhou Y, Gottesman S. 2006. Modes of regulation of RpoS by H-NS. J Bacteriol 188:7022–7025. https://doi.org/10.1128/JB.00687-06.
53. Haeusser DP, Hoashi M, Weaver A, Brown N, Pan J, Sawitzke JA, Thomason LC, Court DL, Margolin W. 2014. The Kil peptide of bacteriophage λ blocks *Escherichia coli* cytokinesis via ZipA-dependent inhibition of FtsZ assembly. PLoS Genet 10:e1004217. https://doi.org/10.1371/journal.pgen.1004217.